Acta Chemica Scandinavica A 31 (1977) 517—529

High Temperature Studies of Marcasite and Arsenopyrite Type Compounds

ARNE KJEKSHUS and TROND RAKKE

Kjemisk Institutt, Universitetet i Oslo, Blindern, Oslo 3, Norway

High temperature investigations by X-ray diffraction, DTA, and quenching experiments have been carried out on $FeAs_2$, $FeSb_2$, $CoAs_2$, $CoSb_2$, $RhAs_2$, $RhSb_2$, $RhBi_2$, $IrAs_2$, $IrSb_2$, $Fe_{0.5}Ni_{0.5}As_2$, $Fe_{0.5}Ni_{0.5}Sb_2$, $NiAs_2$, and $NiSb_2$. The thermal properties of these compounds are discussed in relation to the arsenopyrite *versus* marcasite type structure.

Some two hundred binary and ternary transition metal (T) compounds of the main group V and VI elements (X) take the structure types FeS_2-p (p = pyrite), FeS_2-m (m = marcasite) and/or FeAsS (arsenopyrite; binary prototype $CoSb_2$). A substantial amount of the literature on the subject covers geological aspects or deals with various properties of individual compounds. However, an additional interest stems from their apparent suitability as model substances for bonding considerations. This interest may be based on several motives, their simplicity in atomic architecture and mutual structural resemblance (*cf.*, *e.g.*, Refs. 1, 2, and references therein) being probably the most important.

Features of the relations between the FeS_2-p and FeS_2-m types are presented in recent communications.[1,3] The structural resemblance between the $CoSb_2$ and FeS_2-m types is even more pronounced, and the former can be regarded as a slightly distorted variant of the latter. For the translational symmetry of the lattice the actual deformations are so small that prior to 1955, binary representatives of the $CoSb_2$ type were erroneously classified among the FeS_2-m type compounds. The atomic arrangements correspond similarly [4] and transitions between the two structure types may accordingly be expected as functions of composition, temperature, and/or pressure. In fact, gradual transitions from the $CoSb_2$ to the FeS_2-m type have been accomplished in ternary series $T_tCo_{1-t}X_2$ (T = Fe, Ni; X = As, Sb) [2,5,6] as a function of the compositional parameter t.

At normal temperatures and pressures, binary $CoSb_2$ type compounds have exclusively been found for Co, Rh, and Ir in combination with P, As, Sb, or Bi. This apparent constraint on the $CoSb_2$ type structure compared with the widespread occurrence (in relation to the Periodic System) of compounds with the FeS_2-p and FeS_2-m types, provokes the question of what happens to the $CoSb_2$ type at higher temperatures. An answer to this question could also provide further insight into the occurrence of the various classes A, A/B, and B (*vide infra*) of the FeS_2-m type. Elaboration of the latter point has led to a parallel study of representative FeS_2-m type compounds. Thus, the compounds subject to this study are:

A(FeS_2-m):	$FeAs_2$, $FeSb_2$
B(FeS_2-m):	$NiAs_2$, $NiSb_2$
A/B(FeS_2-m):	$Fe_{0.5}Ni_{0.5}As_2$, $Fe_{0.5}Ni_{0.5}Sb_2$
A/B($CoSb_2$):	$CoAs_2$, $CoSb_2$, $RhAs_2$, $RhSb_2$, $RhBi_2$, $IrAs_2$, $IrSb_2$

where the assigned classifications (see Ref. 7) relate to the room temperature, unit cell proportions.

EXPERIMENTAL

The first preparational step consisted in heating appropriate amounts of the respective elements [turnings from 99.99+ % Fe, 99.999 % Co, and 99.995 % Ni rods, 99.99 % Rh and 99.99 % Ir powders (all from Johnson, Matthey & Co.), 99.999 % As and 99.9995 % Sb (Koch-Light Laboratories), and 99.99+ % Bi (American Smelting and Refining Co.)] in evacuated, sealed silica tubes. The $FeAs_2$ and $NiAs_2$ (*viz.* β-$NiAs_2$) samples were treated as described previously [8] [the "low temperature" modification, α-$NiAs_2$, was readily made by a 2×14 days reaction period (intervening crushing) from NiAs + As at 550 °C], but for the preparations of the other compounds, some modifications of earlier procedures were adopted.

The alterations introduced for $FeSb_2$, $CoSb_2$, and $NiSb_2$ consisted in the initial preparations of the phases FeSb, CoSb, and NiSb by high temperature (1200 – 1000 °C) treatments. The samples were ground to fine powders, appropriate amounts of Sb added, and subsequently annealed once ($CoSb_2$) or twice (intervening crushing) at 700 ($FeSb_2$), 900 ($CoSb_2$), or 600 °C ($NiSb_2$). The $FeSb_2$ and $CoSb_2$ samples were slowly cooled to 600 °C. These simple alterations have thus eliminated the rather time-consuming grinding and annealing cycles earlier used.[4,9]

$CoAs_2$, $RhAs_2$, $RhSb_2$, $IrAs_2$, and $IrSb_2$ were made essentially as described in Ref. 4. On turning to higher maximum temperatures, *viz.* 1000 ($CoAs_2$) or 1200 °C, the overall annealing periods and number of intervening crushings could be reduced appreciably (to 2×2 days). All samples were slowly cooled to 600 °C.

$RhBi_2$ was obtained after reaction at 750 °C (2 days), followed by grinding and annealing at 400 °C (1 month). Renewed attempts to prepare $CoBi_2$ and $IrBi_2$ (*cf.* Ref. 10) were in vain as also reported in, *e.g.*, Ref. 4.

The ternary samples, $Fe_{0.5}Ni_{0.5}As_2$ and $Fe_{0.5}Ni_{0.5}Sb_2$, were made from the binary end members. $Fe_{0.5}Ni_{0.5}As_2$ is readily made by two successive annealings at 740 °C, followed by slow cooling to 600 °C. $Fe_{0.5}Ni_{0.5}Sb_2$ is, however, somewhat more difficult to make. The maximum temperature in the annealing process must not exceed 640 °C (*vide infra*) and equilibrium is attained rather slowly below this temperature. Of the numerous attempts to prepare pure $Fe_{0.5}Ni_{0.5}Sb_2$, none of the samples could be handled identically with respect to annealing time and number of intervening crushings. Further work on the synthetic and other properties of the Fe – Ni – Sb system is in progress.

The temperature of the furnaces surrounding the specimens was kept constant to within ±0.5 °C during the annealing processes, using Getrosist (Philips) temperature regulators and Frigistor reference chambers for the cold points of the Pt/Pt-Rh thermocouples. The recorded annealing and quenching temperatures were measured separately with calibrated Pt/Pt-Rh thermocouples. The silica capsules were made as short as possible in order to minimize effects of thermal gradients in the furnaces, and thin-walled ampoules were utilized for quenching experiments in order to ensure fast cooling rates. The quenching experiments were performed with or without shattering the silica ampoules (depending on the quenching rate required) when brought into contact with ice-water.

Room temperature X-ray powder diffraction data were obtained in a Guinier camera ($CuK\alpha_1$ radiation, KCl as internal standard) and unit cell dimensions derived by applying the method of least squares. All samples were also examined by metallographic methods.

DTA data were collected with a Mettler Recording Vacuum Thermoanalyzer, using ~60 mg samples in sealed silica crucibles (Pd powder as reference). High temperature X-ray powder photographs were obtained in a Unicam camera ($CuK\alpha$ radiation) with the samples sealed in thin-walled silica capillaries. The temperature of the furnace surrounding the specimen was kept constant to within ±5 °C during the exposures. The Pt/Pt-Rh thermocouples of the furnace were calibrated with a standard sample (Ag) in the range 22 to 900 °C. The Guinier data were used to correct the Unicam photographs and least squares refinements were subsequently applied.

A General Electric powder X-ray diffractometer ($CuK\alpha$ radiation, diamond powder as internal standard) with cryostat attachment was used to collect X-ray powder data below room temperature.

RESULTS AND DISCUSSION

(*i*). *$FeAs_2$, $FeSb_2$, $NiAs_2$, and $NiSb_2$.* The high temperature X-ray diffraction data (Fig. 1) show that the FeS_2-*m* type structures of $FeAs_2$, $FeSb_2$, β-$NiAs_2$, and $NiSb_2$ persist until the samples decompose peritectically according to $TX_2 \rightarrow TX + \text{liq.}$, where TX represents phases with NiAs/MnP type structure. The actual temperatures for these reactions are 1014 ± 7, 745 ± 4, 852 ± 5, and 620 ± 2 °C for $FeAs_2$, $FeSb_2$, $NiAs_2$, and $NiSb_2$, respectively, as determined by DTA and quenching experiments.

For $FeSb_2$ and $NiSb_2$ these results are in agreement with those reported in Refs. 11, 12. (Redetermined values for the temperature of the eutectic between TSb_2 and Sb are 628 ± 2 and 616 ± 2 °C for T = Fe and Ni, respectively.) The results for $FeAs_2$ and $NiAs_2$ are, on the

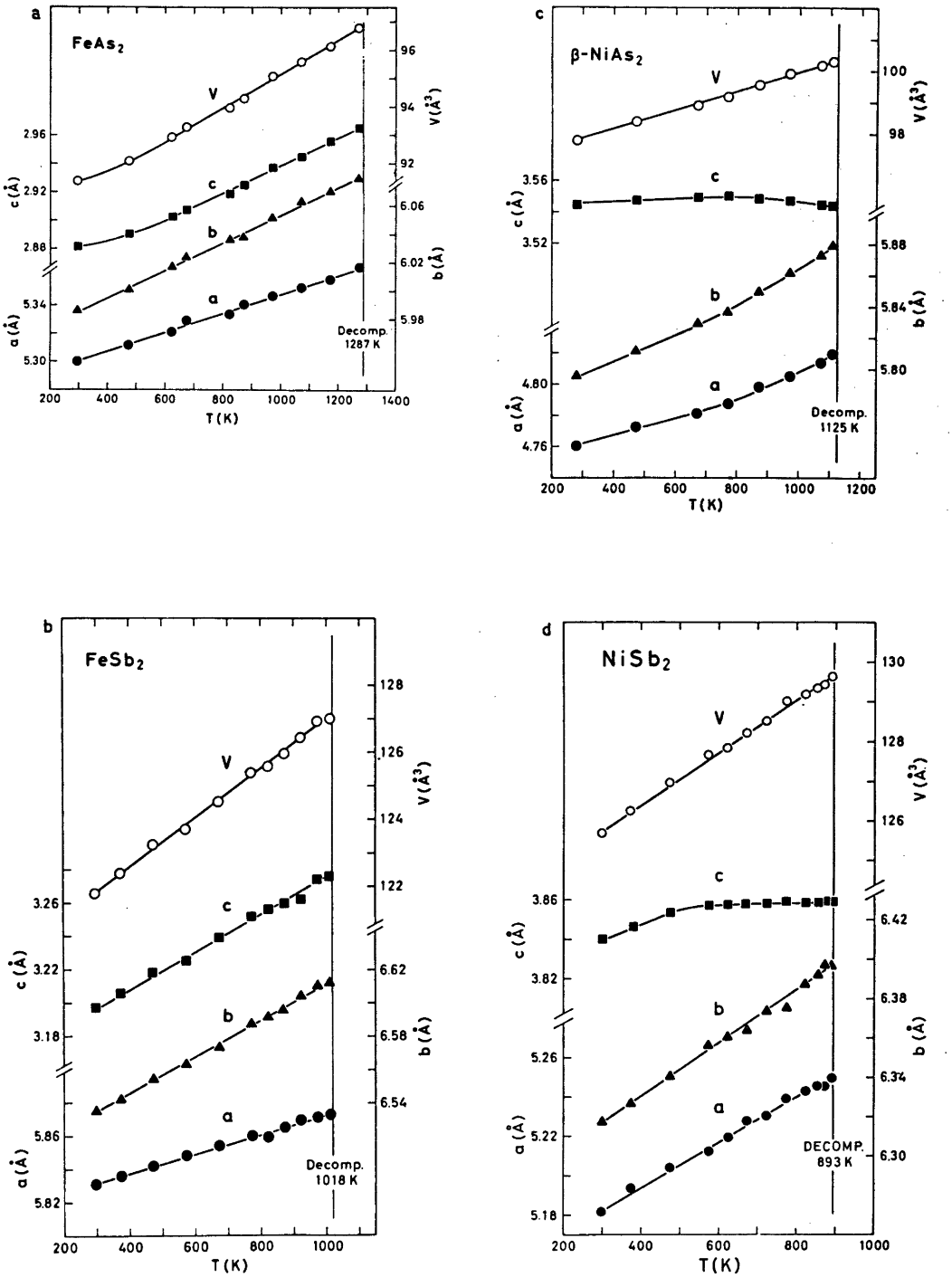

Fig. 1. Thermal expansion of: (a) $FeAs_2$, (b) $FeSb_2$, (c) β-$NiAs_2$ and (d) $NiSb_2$.

other hand, at variance. The reported [12] temperature for the decomposition of $FeAs_2$ is in agreement with the present determination, but the interpretation differs: melting *versus* peritectic reaction. As a support for peritectic reaction, FeAs is detectable on the high temperature X-ray diagrams taken above 1014 °C. For $NiAs_2$ the temperature 852 °C is interpreted in Ref. 12 as representing an eutectic between NiAs and $NiAs_2$, and it is also reported that $NiAs_2$ decomposes (melts) above 1040 °C. According to the present results, $NiAs_2$ disappears at 852 °C, leaving NiAs and liquid. The equilibrium vapour pressures at these high temperatures disturb the sensitivity of the methods and further investigations are needed to find the cause of the discrepancy between Ref. 12 and the present results.

The only minor thermal effect on the *c* axes for the two class B type compounds, β-$NiAs_2$ and $NiSb_2$, is notable. The fact that the thermal expansion of *c* is considerably less than for *a* and *b* has also been observed [3] for other class B, FeS_2-*m* type compounds (particularly for $FeSe_2$ and $FeTe_2$). The class A compounds exhibit, on the other hand, comparable thermal expansions for all axes.

Quenching experiments (followed by room temperature X-ray analyses) from selected temperatures on samples with different nominal compositions, show that the unit cell dimensions are invariant both with respect to temperature and compositions. Hence (using also inferences from Ref. 9), we conclude that the compounds exhibit no appreciable ranges of homogeneity on either side of the TX_2 composition.

Below the temperatures of decomposition (see above), quenched samples demonstrated various degrees of "partial decompositions" $TX_2(s) \rightleftharpoons TX(s) + X(g)$. This is particularly noticeable for $NiAs_2$ which, moreover, also exhibits an $\alpha \rightleftharpoons \beta$ transition (*cf.* Refs. 13, 14;

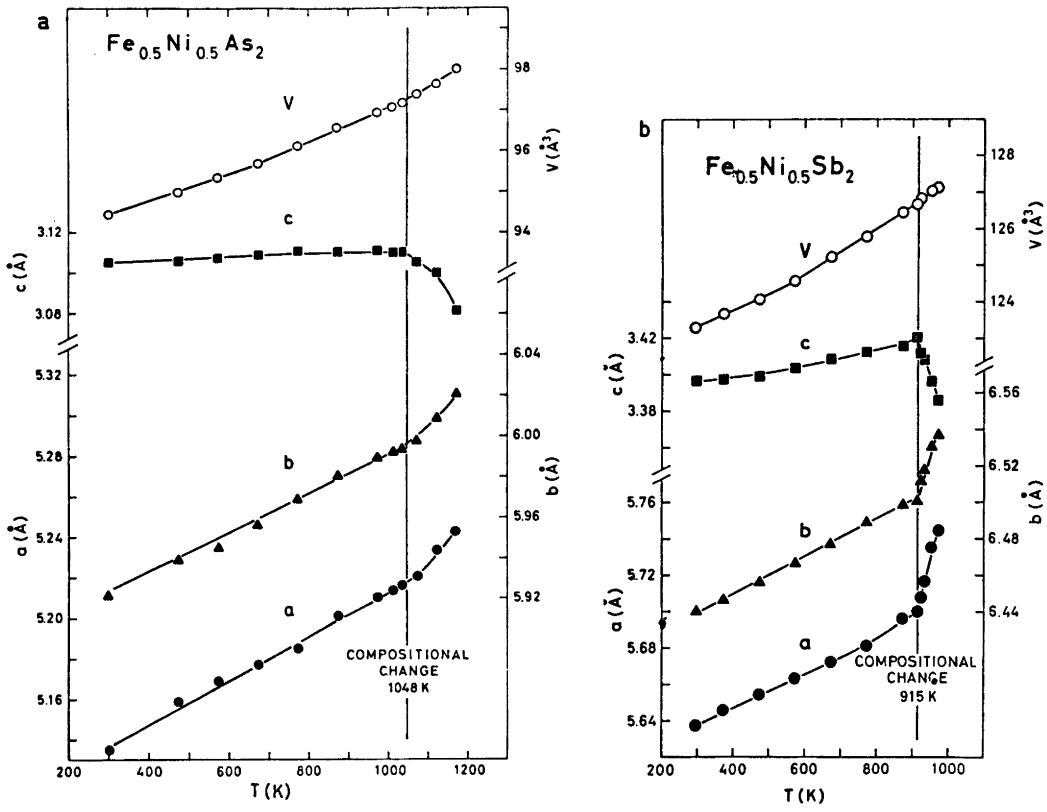

Fig. 2. Unit cell dimensions of: (a) $Fe_{0.5}Ni_{0.5}As_2$ and (b) $Fe_{0.5}Ni_{0.5}Sb_2$ as functions of temperature.

a third, high pressure-high temperature induced, modification with the FeS_2-*p* type structure is also known [15,16]). The reaction $\beta \rightarrow \alpha$ is so slow even at 560 °C that, once β-$NiAs_2$ is formed it persists with no detectable changes (at 560 °C) up to ~60 days before the first traces of α-$NiAs_2$ [orthorhombic; $a = 5.772(2)$, $b = 5.834(2)$, and $c = 11.420(7)$ Å] is detectable. Conversely, the reaction $\alpha \rightarrow \beta$ is also kinetically hampered below 600 °C, whereas complete conversion is rapidly attained above 640 °C. A number of quenching experiments on α- and β-$NiAs_2$ between 560 and 590 °C establish the transformation temperature as 580 ± 4 °C. (The conversion rate for $\beta \rightarrow \alpha$ can be accelerated by adding excess As to β-$NiAs_2$, thus suggesting that the reaction is not of the solid state type but involves the vapour phase, *cf.* Ref. 3.)

Inspired by the existence of α-$NiAs_2$, long term syntheses of $NiSb_2$ (from NiSb + Sb) at selected temperatures down to 300 °C were performed with no success in detecting a corresponding modification for $NiSb_2$.

(ii). $Fe_{0.5}Ni_{0.5}As_2$ and $Fe_{0.5}Ni_{0.5}Sb_2$. Data for the class A/B, FeS_2-*m* type representatives $Fe_{0.5}Ni_{0.5}As_2$ and $Fe_{0.5}Ni_{0.5}Sb_2$ are presented in Fig. 2, which show that their *c* axes (like for class B) expand only slightly below 775 and 642 °C, respectively. Above these temperatures, changes of composition occur according to $Fe_{0.5}Ni_{0.5}X_2 \rightarrow Fe_{1-t}Ni_tX_2 + \text{"Ni}X\text{"} + \text{liq.}$ The notation "Ni*X*" refers to an Ni-rich phase with NiAs like structure, whose composition (judged from data for quenched samples) changes with temperature. There may be a variable Fe content and/or a variable *T* to *X* ratio for "Ni*X*", but studies of the FeAs–NiAs and FeSb–NiSb series are needed to resolve this question.

The compositional changes for $Fe_{0.5}Ni_{0.5}X_2$ are, on the other hand, comparatively easy to follow as a function of temperature. Fig. 3 shows the unit cell dimensions of these phases in the samples quenched from various temperatures T_q. By comparison with unit cell dimensions for the $Fe_{1-t}Ni_tX_2$ phases,[2,5,6] it is evident that a gradual decrease of Ni-content occurs with increasing T_q (no indications of non-stoichiometry of these ternary phases being found; suggesting that the problem may be regarded as "pseudo-binary"). The complete disappearance (as judged from X-ray diffraction and metallographic examinations of quenched samples, high temperature X-ray diffraction and DTA) of the FeS_2-*m* type phases occurs at 1014 and 745 °C for $X = As$ and Sb, respectively. (Due to the disturbingly high As pressure, the uncertainty is larger for $Fe_{1-t}Ni_tAs_2$ than for $Fe_{1-t}Ni_tSb_2$.) This fact and the trends for the unit cell dimensions (Fig. 3) strongly suggest that just before the final decomposition, the approximately pure FeX_2 remains.

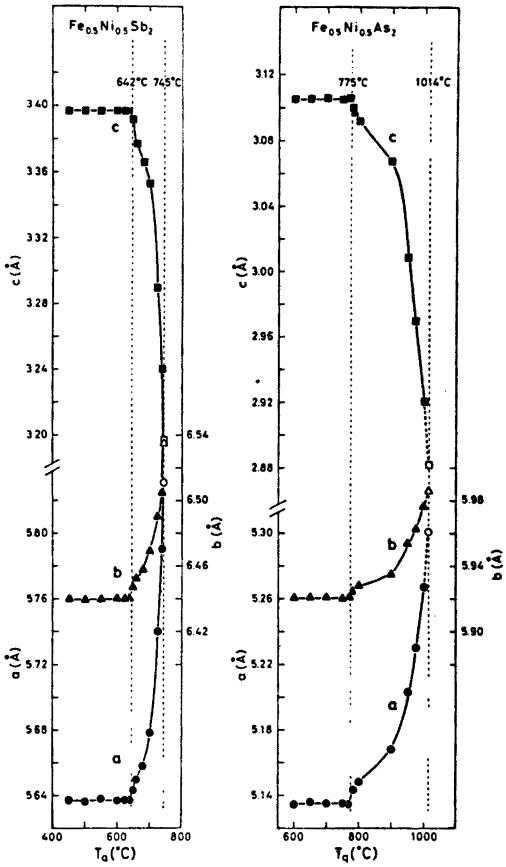

Fig. 3. Room temperature unit cell dimensions for samples of $Fe_{0.5}Ni_{0.5}As_2$ and $Fe_{0.5}Ni_{0.5}Sb_2$ quenched from various temperatures T_q.

The mutual substitution of one kind of atom for another is usually expected to increase with increasing temperature and this has also been suggested for $Fe_{1-t}Ni_tAs_2$.[5] Our results show that this cannot be the case and a more detailed reexamination of the phase relation-

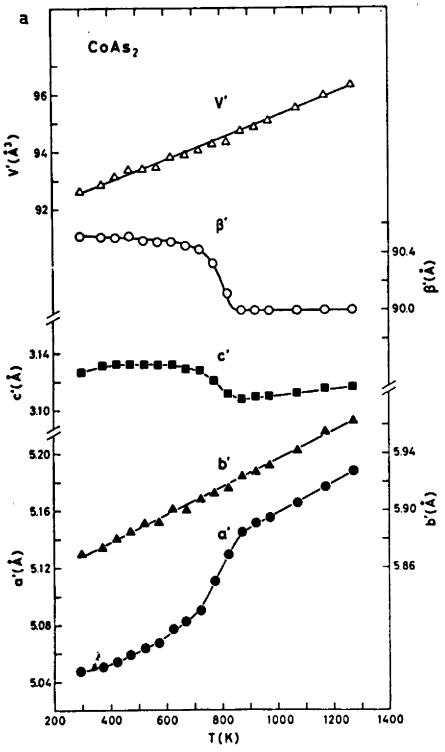
a
CoAs2
V'
β'
c'
b'
a'
V'(Å3)
β'(°)
c'(Å)
b'(Å)
a'(Å)
T(K)

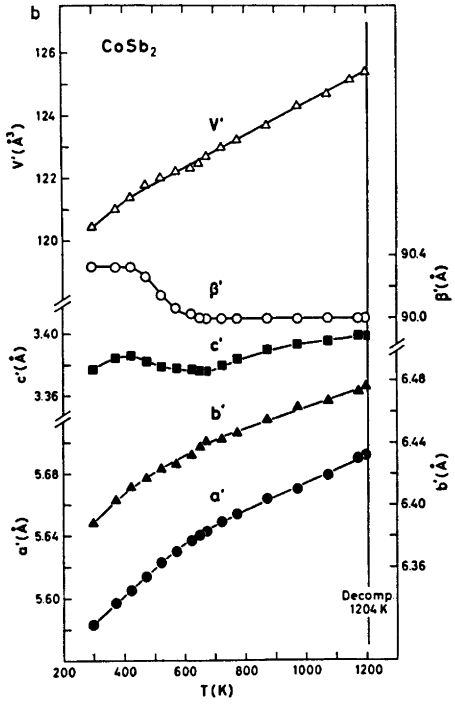
b
CoSb2
V'
β'
c'
b'
a'
Decomp
1204 K
V'(Å3)
β'(°)
c'(Å)
b'(Å)
a'(Å)
T(K)

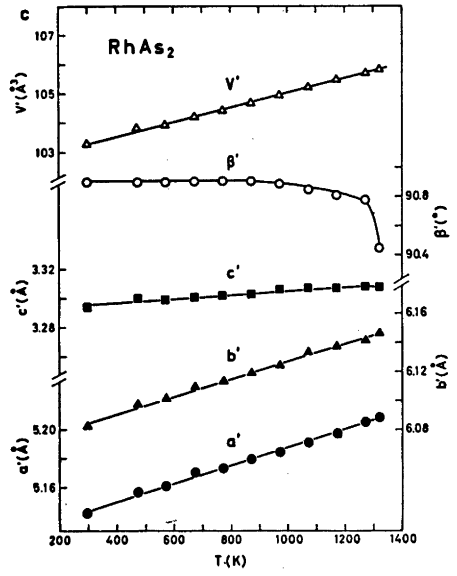
c
RhAs2
V'
β'
c'
b'
a'
V'(Å3)
β'(°)
c'(Å)
b'(Å)
a'(Å)
T(K)

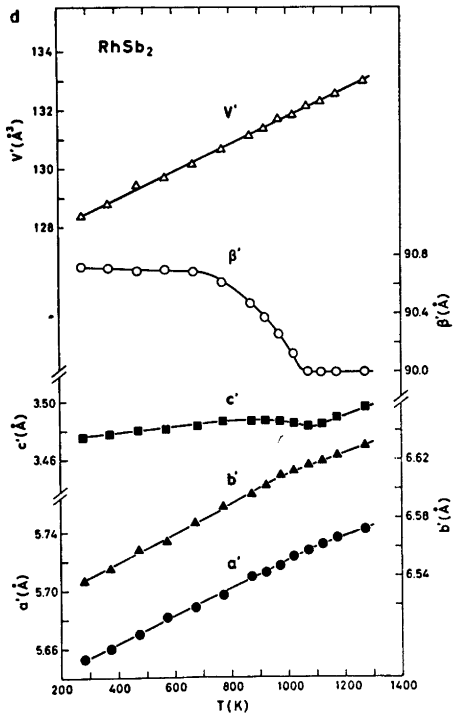
d
RhSb2
V'
β'
c'
b'
a'
V'(Å3)
β'(°)
c'(Å)
b'(Å)
a'(Å)
T(K)

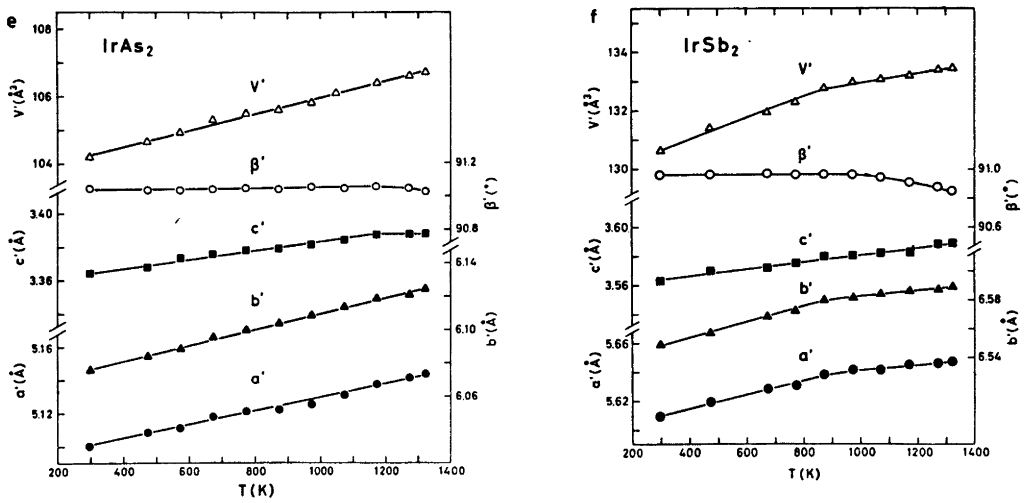

Fig. 4. Pseudo FeS_2-*m* type unit cell dimensions *versus* temperature for (a) $CoAs_2$, (b) $CoSb_2$, (c) $RhAs_2$, (d) $RhSb_2$, (e) $IrAs_2$, and (f) $IrSb_2$.

ships (as a function of temperature) for $Fe_{1-t}Ni_tX_2$ (X = As, Sb) is called for.

(iii). $CoAs_2$, $CoSb_2$, $RhAs_2$, $RhSb_2$, $IrAs_2$, and $IrSb_2$. The scope of the present high temperature X-ray study included, originally, all binary compounds with the $CoSb_2$ type structure. Preliminary attempts showed that the samples of RhP_2 and IrP_2* were difficult to load into the silica capillaries, and examination of these compounds was postponed towards the end of the programme. For reasons given in section *v* they were, however, finally dismissed.

The indexing and reduction of the X-ray diffraction data for $CoSb_2$ type compounds were performed in terms of their true monoclinic unit cells [$\mathbf{a}_{AP}$, $\mathbf{b}_{AP}$, $\mathbf{c}_{AP}$; (β_{AP})], but in order to facilitate comparison with the FeS_2-*m* type compounds, their pseudo FeS_2-*m* type cells [$\mathbf{a}' = (\mathbf{a}_{AP} - \mathbf{c}_{AP})/2$, $\mathbf{b}' = \mathbf{b}_{AP}$, $\mathbf{c}' = (\mathbf{a}_{AP} + \mathbf{c}_{AP})/2$; ($\beta'$)] are conveniently used in the following presentation.

As evident from Fig. 4, $CoAs_2$, $CoSb_2$, and $RhSb_2$ apparently exhibit transformations from monoclinic to orthorhombic symmetry at 870, 650, and 1070 K, respectively; uncertainties being difficult to estimate (*vide infra*). $RhAs_2$, $IrAs_2$, and $IrSb_2$ maintain the monoclinic symmetry up to the maximum temperature (~1300 K) of examination. (The peritectic decomposition of $CoSb_2$ at 931 ± 5 °C is significantly higher in temperature than reported in Ref. 17. This is also the case for $CoSb_3$ which undergoes the peritectic decomposition at 876 ± 5 °C according to the present finding.)

The gradual structural changes as a function of temperature for the compounds under consideration are completely reproducible and do not vary, *e.g.*, with the heating procedure of the samples in the X-ray equipment. Quenching experiments confirm that no appreciable ranges of homogeneity can exist for these TX_2 compounds.[4] The crystalline perfection of samples quenched from temperatures where the high temperature X-ray data show that the orthorhombic symmetry prevails, is compatible with data for samples quenched from the monoclinic temperature region. (The orthorhombic state of these samples is not quenchable.) Hence, non-equilibrium crystal imperfections cannot be the cause of the observed gradual changes for $CoAs_2$, $CoSb_2$, and $RhSb_2$. The results in Fig. 4 must therefore imply that these compounds undergo phase transitions of second or higher order (see *v*). An anomaly in the thermal expansion curves of *c* is a common feature for all these transitions.

* Attempted syntheses of CoP_2 failed, the reaction product being invariably CoP and CoP_3.

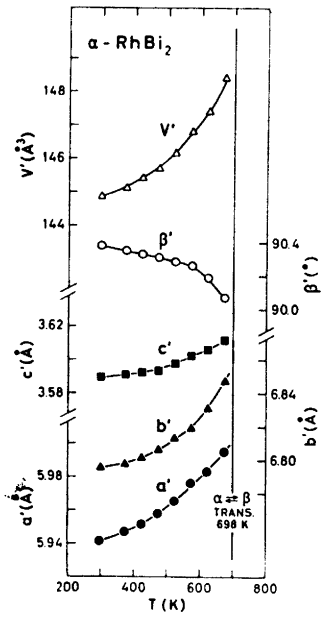

Fig. 5. Pseudo FeS_2-*m* type unit cell dimensions for α-$RhBi_2$ as function of temperature.

(*iv*). *$RhBi_2$*. The $\alpha \rightleftharpoons \beta$ transition in $RhBi_2$ ($\alpha \rightarrow \beta$ detectable on DTA, β-$RhBi_2$ quenchable) is established at 425 ± 3 °C (from DTA and quenching experiments). Peritectic decomposition of β-$RhBi_2$ to RhBi (NiAs type structure) and liquid occurs at 778 ± 4 °C. These results are in perfect agreement with those in Ref. 12.

The thermal expansion of α-$RhBi_2$ (Fig. 5) reveals that β' gradually approaches 90°. Despite numerous additional X-ray photographs taken around 425 °C, the condition $\beta' = 90°$ was never observed. The thermal expansion of c for α-$RhBi_2$ differs from those for $CoAs_2$, $CoSb_2$, and $RhSb_2$ in that the former compound shows no anomaly. Hence, we conclude that the first order phase change $\alpha \rightarrow \beta$ occurs (just) before the structure becomes orthorhombic. Knowledge about the actual atomic arrangement of β-$RhBi_2$ will be needed in order to understand the reason for this odd behaviour.

The structure of β-$RhBi_2$ has been approached,[18,19] but the single crystal data obtained so far have apparently been so poor that the problem remains unsolved. In fact, we were unable to index our X-ray powder data on the basis of the monoclinic unit cell dimensions reported in Refs. 18, 19. Since β-$RhBi_2$ is quenchable, we intend to give the problem continued attention.

(*v*). *$CoSb_2 \rightleftharpoons FeS_2$-m type transformations.* The transformations referred to in section *iii* almost certainly reflect transitions between the $CoSb_2$ and FeS_2-*m* type structures. Unequivocal confirmation of crystallographic changes is difficult in these cases due to the close structural relationship. The angle β' of the pseudo-cell gradually approaches 90° and ultimately, the exact fulfillment of $\beta' = 90°$ becomes virtually indistinguishable from the approximate satisfaction of this condition. Apart from the splitting of certain reflections when $\beta' \neq 90°$, the $CoSb_2$ type diffraction pattern differs from that of FeS_2-*m* also by additional reflections. The intensity of these reflections diminishes rapidly when β' becomes nearly 90°, and their possible presence or absence are even more difficult to detect than the degree of overlap between reflections. The somewhat low quality of the high temperature X-ray powder intensity data prevented clarification of this question through structural refinements. However, semi-quantitative calculations and comparison with relative intensities for $CoAs_2$ *versus* $Fe_{0.5}Ni_{0.5}As_2$ and $CoSb_2$ *versus* $Fe_{0.5}Ni_{0.5}Sb_2$ show that the FeS_2-*m* type is at least a very good approximation to the high temperature structures of $CoAs_2$ and $CoSb_2$. We believe that the same applies to $RhSb_2$.

The $CoSb_2 \rightleftharpoons FeS_2$-*m* type transition may accordingly be regarded as experimentally well established for $CoAs_2$, $CoSb_2$, and $RhSb_2$. The fact that these transitions are of second or higher order contradicts the prediction of Goodenough [20] and emphasizes an important distinction between the $CoSb_2 \rightleftharpoons FeS_2$-*m* and $VO_2 \rightleftharpoons TiO_2$-*r* (*r* = rutile) type transitions.

It appears appropriate to ask why $RhAs_2$, (α-$RhBi_2$,) $IrAs_2$, and $IrSb_2$ do not show corresponding $CoSb_2 \rightleftharpoons FeS_2$-*m* type transitions. The answer to this question is clearly hidden in the parameters (including those specifying the thermal movements of the atoms) which describe the distortion of the $CoSb_2$ type relative to the FeS_2-*m* type structure. Since both structure types comprise a number of parameters (see *vi*), it is difficult to find a satisfactory, general approach to this problem. However, β' can probably be regarded as a parameter

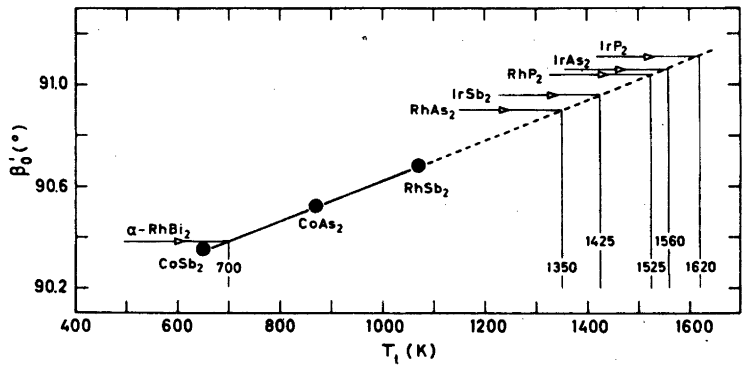

Fig. 6. Room temperature values β_0' *versus* $CoSb_2 \rightleftharpoons FeS_2$-*m* type transition temperature T_t for $CoAs_2$, $CoSb_2$, and $RhSb_2$.

describing the average degree of distortion between the $CoSb_2$ and FeS_2-*m* type structures. In line with this, Fig. 6 shows a linear empirical correlation between the $CoSb_2 \rightleftharpoons FeS_2$-*m* type transition temperature T_t (for $CoAs_2$ $CoSb_2$, and $RhSb_2$) and the room temperature values β_0' of β'. Assuming that this correlation applies to all compounds with the $CoSb_2$ type structure, α-$RhBi_2$ should undergo the $CoSb_2 \rightleftharpoons$ FeS_2-*m* type transition at about 700 K (*i.e.* very nearly at the same temperature as found for the $\alpha \rightleftharpoons \beta$ transition). According to the same correlation, the remaining $CoSb_2$ type compounds should transform to the FeS_2-*m* type above 1300 K. This was, in fact, the reason why RhP_2 and IrP_2 were finally dismissed from the high temperature X-ray programme (*vide supra*).

In the same way that compounds possessing the $CoSb_2$ type structure at room temperature convert to the FeS_2-*m* type at higher temperatures, it is feasible (but less likely) that those of the latter type could show the opposite transition at lower temperatures. Thus, $FeAs_2$, $NiAs_2$, $NiSb_2$, $Fe_{0.5}Ni_{0.5}As_2$, and $Fe_{0.5}Ni_{0.5}Sb_2$ were examined by X-ray diffraction down to 4 K. None of the X-ray diagrams gave, however, indication of (partial or complete) FeS_2-*m*→$CoSb_2$ type transformation. This finding concurs with previous results for $CrSb_2$ and $FeSb_2$.[21] Again the somewhat unique character (*viz.* in relation to the Periodic System) of $CoSb_2$ type compounds is evident.

(*vi*). *The $CoSb_2$ versus the FeS_2-m type structure.* A complete structural description of a crystalline solid involves specification of positions and movements of the atoms relative to each other. Although this problem can be approached in several ways, the conventional crystallographic scheme entirely dominates the field. (A discussion of the $CoSb_2$ and FeS_2-*m* type geometry in terms of alternative variables will be presented in a forthcoming paper.) Following the traditional scheme, a geometrical description of the FeS_2-*m* type structure [space group *Pnnm*; *T* in 2(*a*), *X* in 4 (*g*)] requires the knowledge of three axes (*a*, *b*, *c*) and two positional parameters (x, y), whereas the $CoSb_2$ type [space group $P2_1/c$; $4T$, $4X_I$, and $4X_{II}$ in 4 (*e*)] demands three axes (a_{AP}, b_{AP}, c_{AP}), one angle (β_{AP}), and nine positional parameters (x_T, y_T, z_T, x_I, y_I, z_I, x_{II}, y_{II}, z_{II}).

Since the space group of the $CoSb_2$ type is a subgroup of that for the FeS_2-*m* type, the latter can be converted to a $CoSb_2$ type setting with a_{AP} ($= c_{AP}$), b_{AP}, and β_{AP} specifying the unit cell, and $x_T = 1/4, y_T = 0, z_T = 1/4, x_I = 1/4 + x/2, y_I = y$, $z_I = 1/4 - x/2$, $x_{II} = 1/4 - x/2$, $y_{II} = 1 - y$, and $z_{II} = 1/4 + x/2$ for the positional parameters. Hence, the $CoSb_2$ *versus* FeS_2-*m* type coordinate relationship can, in terms of the distortion parameters Δx_T, Δy_T, *etc.*, be expressed as

T: $x_T = 1/4 + \Delta x_T$, $y_T = \Delta y_T$, $z_T = 1/4 + \Delta z_T$

X_I: $x_I = 1/4 + x/2 + \Delta x_I$, $y_I = y + \Delta y_I$, $z_I = 1/4 - x/2 + \Delta z_I$

X_{II}: $x_{II} = 1/4 - x/2 + \Delta x_{II}$, $y_{II} = 1 - y + \Delta y_{II}$, $z_{II} = 1/4 + x/2 + \Delta z_{II}$.

In order to judge the magnitude of these distortion parameters, sufficiently accurate values for the positional parameters of class A/B, FeS_2-*m* and $CoSb_2$ type compounds are

required. According to Ref. 22, x and y vary systematically within the FeS_2-m type family. The natural class A/B, FeS_2-m type candidates for such a comparison would be $Fe_{0.5}Ni_{0.5}As_2$ and $Fe_{0.5}Ni_{0.5}Sb_2$ (not yet structurally refined), or the Ru-Pd and Os-Pt analogues (could apparently not be prepared [14]). In the lack of experimental data, it may be argued that average values for $FeAs_2$ *versus* $NiAs_2$ and $FeSb_2$ *versus* $NiSb_2$ will provide useful approximations. (Some support for this assumption is to be found in the approximately linear relationships between x, y and the compositional parameter t in the series $Cr_{1-t}Fe_tAs_2$ and $Cr_{1-t}Fe_tSb_2$.[23]).

The degree of reliability of the structure determinations for the $CoSb_2$ type compounds represents another concern. The large number of positional parameters to be determined makes the results [4] from powder diffraction data unreliable for RhP_2, $RhAs_2$, IrP_2, and $IrAs_2$. The structural data for $CoSb_2$, $RhSb_2$, α-$RhBi_2$, and $IrSb_2$ are indeed obtained by single crystal methods,[24] but the results are apparently not of sufficient quality to justify comparative analyses. One is therefore left with $CoAs_2$ [4] as the only suitable candidate.

A schematic presentation of the relationship between the FeS_2-m and $CoSb_2$ type structures is shown in Fig. 7. The projection shows the positions of the T and X atoms in the FeS_2-m type arrangement (assumed for $Fe_{0.5}Ni_{0.5}As_2$, *vide supra*), whereas the lengths and directions of the arrows give their main displacements in the $CoSb_2$ type cell of $CoAs_2$ (displacements along the projection axis are negligible). The illustration shows that the X atoms are shifted mainly along $\pm(\mathbf{a}-\mathbf{c})$, whereas the T atoms approximately along $\pm(\mathbf{a}/5-\mathbf{c})$. The magnitude of each T displacement is about twice that of each X. (For $CoAs_2$ *versus* $Fe_{0.5}Ni_{0.5}As_2$, $\Delta x_T = 0.02$, $\Delta y_T = 0.00$, $\Delta z_T = 0.03$, $\Delta x_I = \Delta x_{II} = 0.00$, $\Delta y_I = \Delta y_{II} = 0.00$, $\Delta z_I = \Delta z_{II} = 0.02$. Similar relations appear to apply to the $CoSb_2$ type

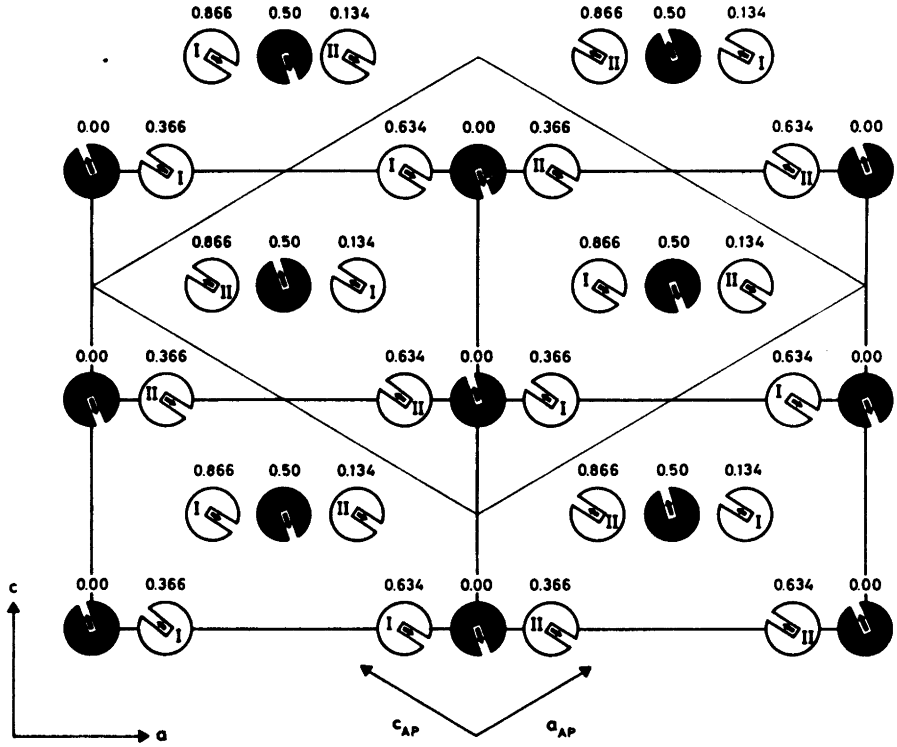

Fig. 7. Relationship between the FeS_2-m and $CoSb_2$ type structures. Filled and open circles represent T and X atoms, respectively, in class A/B, FeS_2-m type arrangement. Lengths and directions of arrows give displacements in order to obtain $CoSb_2$ type atomic arrangement.

antimonides *versus* $Fe_{0.5}Ni_{0.5}Sb_2$.) The net effect of the displacements is that the average $T-X$ distance is kept approximately constant during the transition. A consistent trend is, however, observed in the shifts such that the six approximately equal $T-X$ distances in the FeS_2-*m* type structure are split into three shorter ($T-X_I$) and three longer ($T-X_{II}$) distances in the $CoSb_2$ type (see *viii*).

The FeS_2-*m*⇌$CoSb_2$ type transition (and possibly other transitions originating from the FeS_2-*m* type structure) can be described in terms of the Landau theory.[25] However, a general treatment of this problem is more complicated than for the NiAs⇌MnP or NiAs⇌NbS type transitions,[26] due to the variable positional parameters of the FeS_2-*m* type as opposed to the variable-free NiAs type (in this respect).

(*vii*). *Axial ratios.* Due to differences in absolute dimensions, thermal expansion data are often difficult to compare. In order to facilitate comparison, axial ratios are frequently consulted. For compounds with the FeS_2-*m*

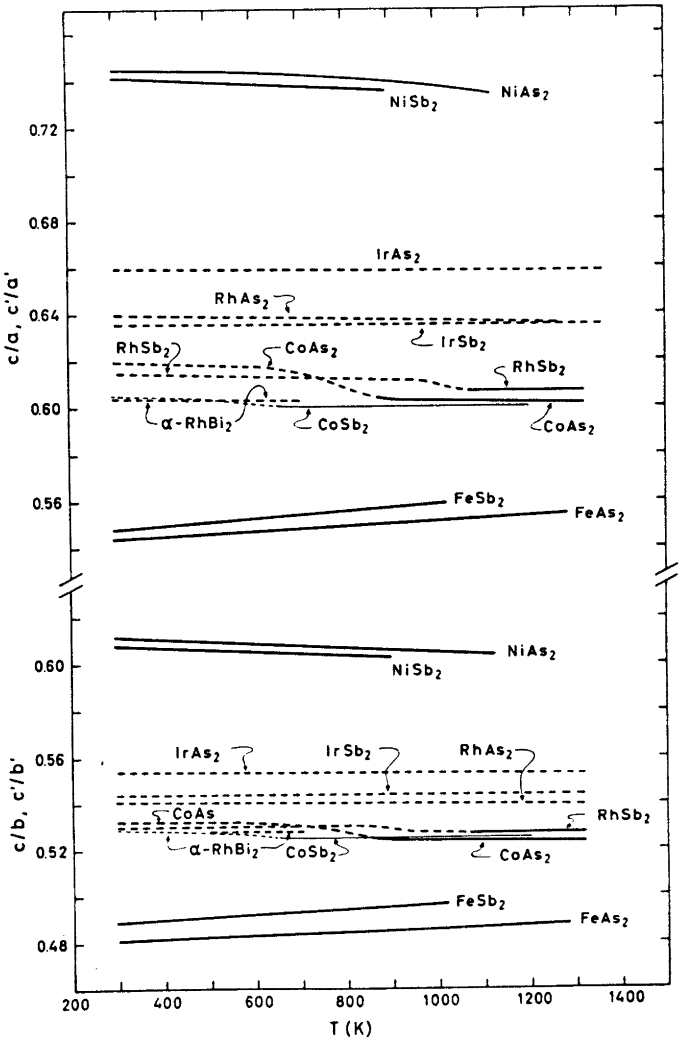

Fig. 8. Axial ratios *c*/*a*, *c*/*b* and *c'*/*a'*, *c'*/*b'* *versus* temperature for FeS_2-*m* and $CoSb_2$ type compounds, respectively. Broken and solid curves correspond to $CoSb_2$ and FeS_2-*m* type regions, respectively.

(and $CoSb_2$) type structure(s), axial ratios have an additional important function in providing the basis for division of the compounds into the classes A, B, and A/B (*vide supra*).

Fig. 8 shows the temperature variation in axial ratios c/a (c'/a') and c/b (c'/b') for the compounds under investigation. Evidently, the class A representatives $FeAs_2$ and $FeSb_2$, exhibit increasing c/a and c/b with increasing temperature, whereas the opposite trend prevails for the class B members β-$NiAs_2$ and $NiSb_2$ (*cf.* also the results for class B, FeS_2-*m* type chalcogenides in Ref. 3). The class A/B, FeS_2-*m* type compounds $Fe_{0.5}Ni_{0.5}As_2$ and $Fe_{0.5}Ni_{0.5}Sb_2$ exhibit c/a, c/b values of 0.605, 0.525 and 0.603, 0.528, respectively, at room temperature and decreases only slightly with increasing temperature (these compounds are, for clarity, not included in Fig. 8). The same applies to the $CoSb_2$ type compounds (class A/B) well below T_t (see *v*) for all members and also from just above T_t for $CoAs_2$, $CoSb_2$, and $RhSb_2$.

The approximate temperature independence of axial ratios for class A/B, FeS_2-*m* or $CoSb_2$ type compounds (neglecting in this connection the $CoSb_2 \rightleftharpoons FeS_2$-*m* type transition regions) is consistent with the increasing and decreasing axial ratios with temperature for the classes A and B, respectively, and also with the idea of class A/B as a "mixture" of the classes A and B (see *viii*). A common decrease in axial ratios is, however, observed in the $CoSb_2 \rightleftharpoons FeS_2$-*m* type transition regions for $CoAs_2$, $CoSb_2$, and $RhSb_2$. (This finding is not a consequence of our neglect to correct c'/a' and c'/b' for $\beta' \neq 90°$ which amounts to a rather minor effect in these cases.) Generalizing from the relative magnitude of the observed decreases for $CoAs_2$ and $CoSb_2$, the changes in axial ratios during the $CoSb_2 \rightleftharpoons FeS_2$-*m* type transitions should be successively smaller (for fixed T atoms) along the sequence: phosphides, arsenides, antimonides, bismuthides. Although the $\alpha \rightleftharpoons \beta$ transition for $RhBi_2$ complicates the situation, it is worth noting that the above observation is consistent with the absence of an anomaly in c (see *iii* and *iv*) and/or a beginning decrease in axial ratios for this compound. Similarly, this finding may also shed new light on the scatter in the room temperature axial ratios for the $CoSb_2$ type compounds: [0.604 (α-$RhBi_2$) $\leq c'/a' \leq$ 0.680(IrP_2), 0.528(α-$RhBi_2$) $\leq c'/b' \leq$ 0.563(IrP_2)], which may be considerably reduced on referring to their (real or hypothetical) FeS_2-*m* type modifications.

(*viii*). *Further aspects.* Previous discussions concerning the relationship between the $CoSb_2$ and FeS_2-*m* type structures have focused attention on that effect of the distortion which produces alternately shorter and longer $T-T$ distances along c'. This "pair formation" and the formal d^5 manifold attributed to T for the $CoSb_2$ type compounds have led a number of workers in the field (*cf.* Refs. 4, 7, 27, and references therein) to suggest that localized, normal $T-T$ σ-bonds are the stabilizing element of the $CoSb_2$ type structure. The rejection of this hypothesis is discussed in Refs. 2, 20 and a few relevant remarks will be made here.

With the attention still focused on the T atoms, it is recognized that six of the twelve $X-T-X$ angles for $CoSb_2$ type compounds show some resemblance to the octahedral angles for class A, FeS_2-*m* type compounds, whereas the other six correspond with those in class B.

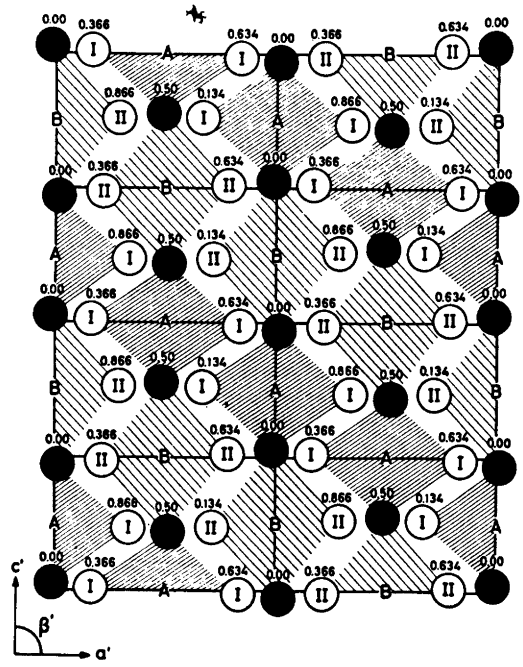

Fig. 9. Arrangement of classes A and B FeS_2-*m* type fragments in the $CoSb_2$ type structure.

However, a simpler and closer similarity between the $CoSb_2$ and the two FeS_2-*m* type classes emerges when attention is shifted to the two crystallographically non-equivalent X_I and X_{II} atoms in the $CoSb_2$ type structure. The immediate coordination ($3T$ and $1X_{II}$) of X_I resembles that for the X atoms in class A, whereas the neighbours ($3T$ and $1X_I$) of X_{II} are arranged as in class B. This aspect is illustrated in Fig. 9, where a distinct pattern of four-membered A and B clusters is evident.

In this pictorial way, the $CoSb_2$ type structure occurs as a natural consequence of mixing equal amounts of structural elements from the FeS_2-*m* type classes A and B. This interpretation lends support to the use of the notation A/B also for the $CoSb_2$ type and reduces in a way the cause of the existence of this structure type to the effects responsible for the distinction between the FeS_2-*m* type classes A and B. Referring to our discussion in Ref. 22 (where we conclude that there is indeed no experimental evidence in favour of a regular type of $T-T$ bonding in class A, FeS_2-*m* type compounds) this observation makes it even more unlikely that the $CoSb_2$ type should be stabilized by normal, localized $T-T$ σ-bonds. This conclusion is also supported by the observed thermal contraction of *c* for $CoAs_2$, $CoSb_2$, and $RhSb_2$ (Fig. 4) during their $CoSb_2 \rightleftharpoons FeS_2$-*m* type transitions. If $T-T$ bonds had been present in their $CoSb_2$ type modifications, the opposite result with an increased *c* would have been expected through relaxation of these bonds.

Without specifying the bonding situation in the FeS_2-*m* and $CoSb_2$ type structures, it seems that the variation in bonding character of the $X-T$ ($T-X$) bonds (*cf.* Ref. 22; the points being elaborated further in a forthcoming paper) is responsible for the occurrence of their different variants A, B, and A/B. The distinct A and B pattern in the $CoSb_2$ type class A/B (Fig. 9) shows that the effects in question occur in a regular, ordered manner, as opposed to the disordered distribution of bonding characteristics in the FeS_2-*m* type class A/B. On this basis, it is only natural that $CoSb_2$ type compounds transform gradually to the class A/B, FeS_2-*m* type structure at higher temperatures by increasing disordering of bonding characteristics.

REFERENCES

1. Kjekshus, A. and Rakke, T. *Struct. Bonding (Berlin) 19* (1974) 85.
2. Kjekshus, A. and Rakke, T. *Acta Chem. Scand. A 28* (1974) 1001.
3. Kjekshus, A. and Rakke, T. *Acta Chem. Scand. A 29* (1975) 443.
4. Kjekshus, A. *Acta Chem. Scand. 25* (1971) 411.
5. Roseboom, E. H. *Am. Mineral. 48* (1963) 271.
6. Bjerkelund, E. and Kjekshus, A. *Acta Chem. Scand. 24* (1970) 3317.
7. Brostigen, G. and Kjekshus, A. *Acta Chem. Scand. 24* (1970) 2983.
8. Kjekshus, A., Rakke, T. and Andresen, A. F. *Acta Chem. Scand. A 28* (1974) 996.
9. Holseth, H. and Kjekshus, A. *Acta Chem. Scand. 22* (1968) 3273.
10. Zhuravlev, N. N. and Smirnova, E. M. *Sov. Phys. Crystallogr. 10* (1966) 694.
11. Hansen, M. and Anderko, K. *Constitution of Binary Alloys*, McGraw-Hill, New York 1958.
12. Shunk, F. A. *Constitution of Binary Alloys, Second Supplement*, McGraw-Hill, New York 1969.
13. Yund, R. A. *Econ. Geol. 56* (1961) 1273.
14. Bennett, S. L. and Heyding, R. D. *Can. J. Chem. 44* (1966) 3017.
15. Donohue, P. C., Bither, T. A. and Young, H. S. *Inorg. Chem. 7* (1968) 998.
16. Munson, R. A. *Inorg. Chem. 7* (1968) 389.
17. Elliott, R. P. *Constitution of Binary Alloys, First Supplement*, McGraw-Hill, New York 1965.
18. Zhuravlev, N. N. and Zhdanov, G. S. *Soviet Phys. JETP 1* (1955) 91.
19. Kuz'min, R. N. and Zhuravlev, N. N. *Sov. Phys. Crystallogr. 6* (1961) 209.
20. Goodenough, J. B. *J. Solid State Chem. 5* (1972) 144.
21. Holseth, H., Kjekshus, A. and Andresen, A. F. *Acta Chem. Scand. 24* (1970) 3309.
22. Kjekshus, A., Rakke, T. and Andresen, A. F. *Acta Chem. Scand. A 31* (1977) 253.
23. Kjekshus, A., Peterzéns, P. G., Rakke, T. and Andresen, A. F. *To be published.*
24. Zhdanov, G. S. and Kuz'min, R. N. *Sov. Phys. Crystallogr. 6* (1962) 704.
25. Landau, L. D. and Lifshitz, E. M. *Statistical Physics*, Pergamon, London 1969.
26. Franzen, H. F., Haas, C. and Jellinek, F. *Phys. Rev. B 10* (1974) 1248.
27. Jeitschko, W. and Donohue, P. C. *Acta Crystallogr. B 31* (1975) 574.

Received March 31, 1977.